ION CYCLOTRON RESONANCE HEATING IN THE WISCONSIN SUPPORTED TOROIDAL OCTUPOLE

by

J. D. Barter and J. C. Sprott

Plasma Studies PLP 710

University of Wisconsin

COO-2387-82

ION CYCLOTRON RESONANCE HEATING IN THE WISCONSIN SUPPORTED TOROIDAL OCTUPOLE*

by

J. D. Barter and J. C. Sprott

University of Wisconsin Physics Department

Madison, Wisconsin 53706 USA

ABSTRACT

Ion heating at the fundamental of the cyclotron resonance ($1\text{MHz} \lesssim \frac{\omega}{2\pi} \lesssim 3\text{MHz}$) in a toroidal octupole magnetic field is found to be in good agreement with single particle, cold plasma theory at power levels $p_{abs} \lesssim 100$ kW ($E \lesssim 100\text{V/m}$) and ion temperatures $kT_i \lesssim 600\text{eV}$. Good penetration of the electric field is observed in the densest available plasmas ($n \sim 7 \times 10^{12}$ cm^{-3}) with no evidence of parametric decay or enhanced particle loss other than temperature dependent losses such as thermal flow to obstacles. Ion temperatures are limited by charge exchange on the large neutral reflux at the higher rf powers.

INTRODUCTION

Wave heating in the ion cyclotron range of frequencies is becoming a recognized means of supplemental heating for tokamaks and other devices (Rothman, et al., 1969; Swanson, et al., 1972; Hosea and Hooke, 1973; Takahashi, et al., 1976; Iiyoshi, et al., 1976; Scharer, et al., 1976; Vdovin et al., 1976).

We report ICRH experiments performed on the supported toroidal octupole at the University of Wisconsin. The study of ICRH in an internal ring device offers advantages over a Tokamak such as the absence of ohmic heating current, and the ability to vary the plasma parameters, especially density and magnetic field over a wide range. For most plasma densities available in the octupole the wavelength at the ion cyclotron frequency ($\lambda \sim$ 100 - 300m) is much larger than the size of the machine. The vacuum electric fields are of linear polarization and point in the toroidal direction perpendicular to the poloidal octupole field. The spatial distribution of these fields is determined mainly by the conducting cavity walls and hoops. The penetration of the electric field can be measured directly in the presence of plasma and can be analytically approximated by placing "image" currents to approximate the distributed currents in the conducting walls.

Both the plasma loading of the rf antenna and the resulting ion temperature are compared to single particle, cold plasma theory with good agreement even at high rf powers when ion gyroradii are no longer small compared to electric field scale lengths. The ion temperature is governed mainly by two loss mechanisms: particle loss to hoop supports and to the ion energy analyzer collector pipe, and charge exchange on the neutral reflux which originates from various vacuum surfaces including the toroidal limiter and fifth hoop insulator. The large neutral reflux dominates the ion losses at the higher rf powers and emphasizes the need for better cleaning techniques.

APPARATUS AND DIAGNOSTICS

The toroidal octupole device on which these experiments have been performed is described by Dory, et al. (1966). A poloidal cross section of the device is shown in figure 1. The four copper hoops of circular cross section are continuous and encircle an iron core (not shown). Currents induced in these hoops by capacitor excitation form the octupole poloidal field with half sine wave duration of either 5 or 10 msec. The maximum available poloidal field at the midpoint of the outer wall is 2.2 kG with fields up to 12 kG near the inner hoops and an octupole null near the minor axis. The poloidal field strength is specified by the voltage to which the capacitors are charged where the maximum field is obtained with a capacitor charge of 5 kV. Toroidal fields up to 5 kG can be added independently but are not used for the experiments described here.

Densities are measured with Langmuir probes, while ion temperatures are measured by extracting ions from the null field region through a ferromagnetic pipe. The extracted ions are analyzed in a 127° curved plate electrostatic analyzer (Erickson, 1970) and counted with a Daly detector (Daly, 1960 a,b).

An rf electric field in the toroidal direction suitable for cyclotron heating in the poloidal field is induced by a "fifth hoop" of oblong cross section mounted near the floor of the aluminum toroid. The single turn fifth hoop is concentric with the four poloidal field hoops but has a gap which is driven externally as a single turn inductor

Since the inductor is an integral part of the tank circuit, any reactive loading presented by the plasma merely shifts the frequency slightly ($\frac{\Delta f}{f} \sim 10^{-3}$ for $n = 5 \times 10^{10}$ cm^{-3}) without affecting the oscillator to plasma coupling appreciably. The fifth hoop has a grounded center tap which increases single turn hoop voltage without increasing insulation requirements. The oscillator (figure 2) is tuned to the range 1 MHz $\lesssim f \lesssim$ 3 MHz and can supply up to $\sim$ 1MW of rf to the tank circuit at 40 kV zero to peak for pulse lengths up to 2 msec.

The inductive electric field of the fifth hoop is purely toroidal and is the field which gives rise to the cyclotron resonance heating. The electrostatic fields are not toroidal in general and must be shielded from the plasma with a Faraday shield and toroidal limiter if the plasma load to the fifth hoop arising from the ion cyclotron heating is to be measured. This hoop loading is measured by sampling both the rf voltage and drive current applied to the fifth hoop tank circuit. Comparison of the values with and without plasma gives the power applied to the plasma. Due to the voltage limitations imposed by the shield, the hoop is normally used only with a glass cover for insulation from the plasma.

The octupole magnetic field is shown in figure 3. The light lines indicate flux lines while heavy lines indicate loci of constant magnetic field strength ($|\vec{B}|$ = constant), arbitrarily normalized to one at the outer wall midplane. Both flux lines and $|\vec{B}|$ lines form toroidal surfaces of rotation about the major axis. For strongest ion heating the heating frequency and the magnetic field strength are chosen to place the ion cyclotron resonance on a $|\vec{B}|$ surface

which passes close to the fifth hoop and thus samples the high electric fields near the hoop ($.5 \leq |\vec{B}| \leq 2$). The glass insulation which is shown installed over the fifth hoop also acts as a toroidal limiter for the plasma.

The time evolution of a representative experiment pulse is shown in figure 4. These plots have been generated by a plasma simulation code which will be discussed in section IV. Trace a is the poloidal magnetic field strength measured at the midpoint of the outer wall. The plasma generally used for these experiments is produced by ECRH (Sprott, 1969) in which case power at 2.45 GHz (figure 4b) is provided by a 5 kW cw magnetron driven by a small fraction of the poloidal field current. The plasma density (figure 4c) rises rapidly as soon as the electron cyclotron resonance appears in the machine and seeks a density at which $\omega_{pe} \sim \omega$. In figure 4d the ion temperature rises rapidly when ICRH power is applied. The ICRH pulse is turned on at 5 msec and off at 7 msec. The rise of neutral density (figure 4e) occasioned by the increased bombardment of the walls with high energy ions increases the energy loss by charge exchange. The rising charge exchange loss soon dominates the ion cooling and the ion temperature drops to a level dictated by the neutral reflux.

WAVE PENETRATION

Since the vacuum wavelength at our frequencies (1-3 MHz) is much greater than the machine size, we are well below the minimum cavity mode frequency. In this regime, it is convenient to represent the vacuum rf electric field as the superposition of fields induced by the hoop and several of its images.

The effect of the plasma on the rf electric field and its polarization can be estimated from two view points. First, we look for regions of propagation and evanescence in the toroid. The cold plasma dispersion relation for a bounded plasma (Scharer, et al., 1976)

$$\frac{S}{P} n_{\perp}^4 - (S-n_{\parallel}^2)\, n_{\perp}^2 + (R-n_{\parallel}^2)\,(L-n_{\parallel}^2) = 0$$

in the region $\omega \ll \omega_{ce}$ where ω is the drive frequency, ω_{ce} is the electron cyclotron frequency, R, L, S and P are the dielectric tensor elements defined by Stix (1962) and $n_{\parallel}$ and $n_{\perp}$ are the components of the index of refraction parallel and perpendicular to the static magnetic field. The effects of magnetic field curvature are not included. In the octupole the magnetic field is purely poloidal with relatively strong curvature which we will assume does not seriously alter this qualitative treatment.

The variation of rf electric field strength along the magnetic field can be Fourier analyzed with components specified by an integer m such that the wave number $k_{\parallel} = \frac{2\pi}{\lambda_{\parallel}} = \frac{2\pi m}{L_B}$ where L_B is the length of the magnetic field line. The perpendicular wave number can then be found as a function of position and plasma density. Some surfaces of constant $n_{\parallel}^2$ are shown in figure 5.

The magnetic field increases from zero at the minor axis to a maximum near the hoops. For the case of density constant in space ($n \sim 3 \times 10^{10}$ cm^{-3}) and representative m ($1 \leq m \lesssim 14$) the surface $n_{\parallel}^2 = S$ is approximately coincident with the ion cyclotron resonance ($\omega = \omega_{ci}$) while $n_{\parallel}^2 = R$ falls inside the resonance ($\omega > \omega_{ci}$) and $n_{\parallel}^2 = L$ falls outside the resonance ($\omega < \omega_{ci}$). The slow wave propagates

outside the $n_{\parallel}^2 = S$ surface and becomes weakly evanescent inside. The fast wave is weakly evanescent outside $n_{\parallel}^2 = S$ and becomes strongly evenescent inside $n_{\parallel}^2 = S$. A very narrow band just outside $n_{\parallel}^2 = S$ ($\omega \lesssim \omega_{ci}$) (not shown) also exists in which the fast mode propagates but should not affect the electric field intensity at the ion cyclotron resonance. Since the fast wave is only weakly evanescent (skin depth of several centimeters) and the slow wave propagates to the resonance we may expect linear polarization of the rf electric field at the resonance.

Furthermore, a modified form of the technique developed by Stix (1962) for the analysis of natural modes of a plasma has been used to estimate the extent of elliptical wave polarization near the ion cyclotron resonance. According to this analysis (Barter, 1976) the width of the zone of elliptical polarization should be negligible compared to the ion gyroradius at our plasma densities and temperatures. The polarization should be approximately linear elsewhere except near the electron cyclotron resonance. Thus, we assume a linearly polarized electric field in the region of the ion cyclotron resonance.

The rf electric fields are readily measured with rf magnetic loops both in vacuum and in plasmas up to the densest available ($n = 5.7 \times 10^{12}$ cm^{-3}). In figure 6 is a plot of the vacuum rf electric field vertically above the fifth hoop and again with a dense ($n = 6.7 \times 10^{12}$ cm^{-3}) plasma. The plasma depresses the rf electric field near the B = 0 axis, but the field penetrates well as far as the ion cyclotron resonance. Since the ion heating is proportional to the square of the electric field, the bulk of the heating is done in the high electric field region near the fifth hoop where the penetration is good. For this reason we represent the vacuum fields with an analytical model (solid curve of figure 6) and ignore any plasma effects on the vacuum field.

ION HEATING THEORY AND SIMULATION

With linear field polarization it is convenient to calculate the power absorbed by the plasma per unit volume according to the relation

$$dP/dV = (\vec{\sigma} \cdot \vec{E}) \cdot \vec{E} = \sigma_{\perp} E_{\perp}^2 + \sigma_{\parallel} E_{\parallel}^2$$

and the average power absorbed per ion is:

$$\frac{dW}{dt} = \int \sigma E^2 \, dV / \int n dV$$

where $_{\perp}$ and $_{\parallel}$ refer to directions with respect to the magnetic field. For the conductivity, we use the cold plasma dispersion relation to derive (Wharton, 1965; Sprott, 1969):

$$\sigma_{\perp} = \varepsilon_o \omega_{pi}^2 \nu \left[\frac{\omega^2 + \omega_{ci}^2 + \nu^2}{(\omega^2 - \omega_{ci}^2)^2 + \nu^2(2\omega^2 + 2\omega_{ci}^2 + \nu^2)}\right]$$

and

$$\sigma_{\parallel} = \frac{\varepsilon_o \omega_{pi}^2 \nu}{\omega^2 + \nu^2}$$

where

ε_o = permitivity of free space,

ω_{pi} = ion plasma frequency,

ω = driving frequency,

ω_{ci} = ion cyclotron frequency as a function of B,

ν = effective collision frequency

We shall also assume small collision frequencies for which $\sigma_{\parallel} \to 0$ and since we have set $E_{\parallel} = 0$, we will ignore the heating contribution of $\sigma_{\parallel}$. Further, in the $\nu \to 0$ limit, $\sigma_{\perp}$ can be represented by a delta function in B and we have (Sprott, 1969):

$$\frac{d\overline{W}}{dt} = \frac{e}{2} \frac{\int nE^2 \, \delta(B-B_o) dV}{\int n dV}$$

where B_o is the magnetic field at the ion cyclotron resonance and ($B_o = \frac{M\omega}{e}$) and e is the electronic charge.

As it stands, the theory predicts the average power absorbed per particle for a given excitation voltage (E_o) and frequency (B_o) of the fifth hoop. An example of a test of the theory at this point is shown in figure 7. The plasma load presented to the fifth hoop for a constant electric field strength at the resonance zone is measured vs. the plasma density (x's) and compared to the single particle theory (solid line) which is proportional to density. The agreement is good within the uncertainties of the measurement and the theory. A second estimate of the plasma loading was obtained by measuring the rise time of the heated ion distribution. If a homogeneous ion distribution is assumed, this can be converted to a volume averaged heating. The disagreement of this measurement is probably related to the failure of this assumption.

This theory can also be used to predict the ion temperature achieved if all the competing gain and loss mechanisms in the octupole are considered. A computer code (SIMULT) described by Sprott and Strait (1976) has been used to simulate the time development of the plasmas. This code is a zero dimensional solution of the particle and energy balance equations, in which all known heating and loss mechanisms are included in some appropriately spatially averaged manner. The code predicts the time dependent, spatially averaged, densities and temperatures of both electrons and ions as well as the neutral density (assumed 0.025 eV H_2).

EXPERIMENTAL SCALINGS

An example of a velocity distribution measured by the method of section II is shown in figure 8. The velocity distribution is plotted

against the ion kinetic energy in the plasma. In this example of a high temperature distribution, three distinct regions appear. An unheated component includes ion energies $E_p \leq 250$ eV with a slope $kT_i \approx 150$ eV. The heated component is of approximately equal density and extends to $E_p \leq 1$ keV. Beyond $E_p = 1$ keV a cutoff occurs which is associated with the ion gyroradius limit imposed by the finite amount of magnetic flux in the poloidal field.

The unheated component is continually populated by charge exchange on the neutral reflux. The observed temperature of this component probably appears deceptively high due to the plasma potential oscillations at the driving frequency ($\Delta V_p \approx 100$ V). The ion distribution is also being sampled at the bottom of a magnetic well for which roughly half the particles do not sample the resonance zone. For those ions which do sample the resonance zone, the distribution function is predicted to be Maxwellian (Namba and Kawamura, 1970; Sprott and Edmonds, 1971) and to remain so even in the presence of weakly velocity dependent forces.

We use the slope of the heated component as our measured ion temperature which is then compared to the predictions of SIMULT. The scaling of ion temperature has been measured with respect to various plasma parameters and shows good overall agreement.

In figure 9 the scaling of T_i vs. the zero to peak rf hoop voltage (V_{op}) is compared to SIMULT. The large error bars at low energies arise from the finite energy resolution of the analyzer ($\approx$3 eV) and the oscillating plasma potential driven by the unshielded

hoop ($\simeq$ 5 eV at the low powers). Although absorbed power is proportional to V_{op}^2 the temperature is found to vary approximately as V_{op} at the higher powers due to energy dependent loss to supports which scale as $\sqrt{kT_i}$ (Erickson, 1967) and to charge exchange which scales as the neutral hydrogen pressure and exhibits a peak near kT_i = 3 keV (Rose and Clark, 1961, Sprott and Strait, 1976).

The measured temperature tends to fall above the simulation because of two factors. The simulation calculates a temperature averaged over the plasma volume where the ion energy distribution is assumed to be homogeneous and Maxwellian. However, the distribution is only measured locally and is observed to be non-Maxwellian in general.

The scaling of ion temperature with neutral hydrogen filling pressure is shown in figure 10 compared to SIMULT. The agreement is good and demonstrates primarily the reliability of the charge exchange loss calculation of SIMULT.

In figure 11 the poloidal magnetic field strength is varied while holding the driving frequency constant. This scaling therefore moves the resonance zone with respect to the plasma and the fifth hoop. The data does show the proper trend but doesn't agree well with our simple theory. Again the plasma simulation assumes an homogeneous ion temperature where the resonance heating is averaged over the plasma volume. The movement of the resonance, will, however, affect the power absorbed per flux surface and thus change the spatial distribution of ion energies while the ion sampling position remains fixed.

A change in the shape of the ion velocity distribution is also observed as the poloidal magnetic field capacitor charge is raised above 3.5 kV in figure 10. A transition occurs from a three component distribution as in figure 7 to a single component Maxwellian as the resonance zone moves from a surface near the octupole hoops ($|\vec{B}|$ 1.5, (figure 3) to a surface near the B = 0 axis ($|\vec{B}| > 1$, figure 3). Since the fifth hoop is unshielded, voltages of ~ 20 kV can appear near the edge of the plasma which would bombard the glass insulator with high energy ions and electrons. The bombardment of these surfaces by energetic charged particles releases adsorbed neutrals which travel directly through the resonance zone for the high field cases (B_p capacitor charge $\geq$ 3.5 kV) and account for the smoother ion distributions functions and lower temperatures. Without a pressure gauge with sufficient time and space resolution, this is difficult to verify.

Movement of the resonance zone also places heavy emphasis on the electric field strength off the vertical axis. The regions least well described by our analytical representation are those in the high field regions behind the hoops. The resonance zone samples these regions for low magnetic field (B_p capacitor charge < 3.5 kV in figure 11).

A graphic demonstration of the importance of neutral reflux from the toroid surfaces is shown in figure 12. Here the neutral pressure has been measured long after the experimental pulse and extrapolated back to the time of the end of the ICRH pulse assuming constant pumping speed. The resulting neutral pressure is strongly dependent on the state of cleanliness of the vacuum surfaces. In this figure the increase in neutral pressure varies approximately

as V_{op}^2. The relative magnitude of the losses due to various mechanisms including charge exchange as calculated by SIMULT are shown in figure 13. Even though SIMULT underestimates the magnitude of the neutral reflux (figure 12), charge exchange dominates the loss mechanisms at high values of ICRH power.

Methods for cleaning the toroid surfaces are currently under study. Titanium gettering has been employed on the glass insulator sector which covers the high voltage ends of the fifth hoop. This technique has served to reduce the reflux as measured after the experiment but without significant rise in ion temperature. We also plan to replace the present glass insulator with MACOR machinable ceramic which has been found to be relatively clean when used as limiter material in tokamaks (Bardet et al., 1976). Methods of discharge cleaning including low power ECRH are also being studied.

The simulation program can also be used to account for the power flow in the ICRH system. Figure 14 shows a block diagram of the system for a representative steady state plasma. At the design limit of the oscillator we can supply 830 kW at 39 kV_{op} to the tank circuit. The plasma absorbs 91 kW at the ion cyclotron resonance to produce an ion temperature of 480 eV in a plasma of 2×10^{11} cm^{-3} density. Of this power 52% is lost to charge exchange and 45% to obstacles, with the remaining 3% lost by several less important mechanisms. The low coupling efficiency from the oscillator to the plasma is limited by the Q of the tank circuit we are able to construct. In principle the coupling efficiency may be increased either by increasing the tank circuit Q (increasing the parallel resistance of the tank circuit) or increasing the plasma density (lowering the plasma load connected in parallel).

CONCLUSIONS

We have demonstrated that electric fields penetrate well to the ion cyclotron resonance zone even at the highest available densities ($n \lesssim 7 \times 10^{12}$ cm^{-3}).

The single particle cold plasma theory for linear polarized wave heating at the fundamental of the ion cyclotron resonance is shown to describe the observed heating well.

This theory has been tested at two points. First, the power absorbed by the plasma has been compared to the theory since we can measure the spatial distribution of electric field. Second, the resulting ion temperature has been compared to the theory with the help of a plasma simulation code to calculate the simultaneous contributions of many gain and loss mechanisms.

Ion temperatures of roughly half the ion population have been raised from $kT_i \lesssim 3$ eV to $kT_i \lesssim 600$ eV with no deleterious effects other than those explained by the temperature dependent loss mechanisms considered by the simulation code.

The ion temperature is limited at the high rf powers by charge exchange on the neutral reflux. We are exploring methods of controlling the reflux which include titanium gettering of the toroid surfaces and the installation of a MACOR insulator to replace the glass insulator over the fifth hoop.

When a toroidal field is added, we can produce ohmically heated plasmas with currents ~ 20 kA and densities approaching 10^{13} cm^{-3}. We plan to pursue fast wave toroidal eigenmode heating experiments in this more Tokamak-like regime.

*This work is supported by U.S. ERDA.

Collaboration with R. J. Groebner on problems of neutral reflux and the assistance of A. P. Biddle with data acquisition have been very helpful. The assistance of T. Lovell with the design and construction of the oscillator is appreciated. We also wish to thank D. Kerst and J. Scharer for helpful discussions.

Fig 1. The Wisconsin supported toroidal octupole.

Fig 2. Oscillator circuit to produce $\lesssim 40$ kV_{op} across centertapped fifth hoop.

Fig 3. Poloidal field structure of the supported toroidal octupole. Light lines indicate magnetic field lines (ψ). Heavy lines indicate loci of constant field strength $|\vec{B}|$. The fifth hoop is shown with its glass insulator in place.

Fig 4. Time development of the typical ICRH experiment from computer simulation.

Fig 5. Poloidal cross section of the octupole showing regions of evanescence (E) and propagation (P) of the slow wave. The fast wave is evanescent everywhere but is only weakly evanescent outside $n_{\parallel}^2 = S$ ($\omega = \omega_{ci}$).

Fig 6. Measured electric field penetration in the supported octupole.

Fig 7. Absorbed power as determined by hoop loading and by observed particle heating rates compared to single particle heating theory.

Fig 8. Ion velocity distribution $f(\vec{v})$ plotted vs. ion energy in the plasma.

Fig 9. Ion temperature vs. applied zero to peak hoop voltage.

Fig 10. Ion temperature vs. H_2 pressure for constant hoop voltage.

Fig 11. Ion temperature vs. poloidal field capacitor charge for fixed rf frequency compared to SIMULT.

Fig 12. Neutral reflux in the presence of ICRH compared to SIMULT.

Fig 13. Relative magnitude of ion energy losses calculated by SIMULT.

Fig 14. ICRH power flow for $V_{op} = 39$ kV.

REFERENCES

1. Bardet R., Bernard M., Brifford G., Clement M., Frank R., Gauthier A., Gregoire M., Gruber S., Grelot P., Hesse M., Parlange F., Pinet D., Porrot E., Rey G., Taquet B., and Weisse J., 1976, EUR-CEA-FC-816.
2. Barter J. D., 1976, Ph.D. thesis, U. of Wisconsin.
3. Barter J. D. and Sprott J. C., 1975, Phys. Rev. Lett., 34, 1607.
4. Daly N. R., 1960, Rev. of Sci. Instr., 31, 264.
5. Daly N. R., 1960, Rev. of Sci. Instr., 31, 720.
6. Dory R. A., Kerst D. W., Meade D. M., Wilson W. E., and Erickson C. W., 1966, Phys. Fluids, 9, 997.
7. Erickson C. W., 1967, Ph.D. thesis, U. of Wisconsin.
8. Erickson C. W., 1970, Phys. Fluids, 13, 819.
9. Hosea J. C. and Hooke W. M., 1973, Phys. Rev. Lett., 31, 150.
10. Iiyoshi A., Obiki T., Sato M., Sasaki A., Mutoh T., Adachi S., Uo K., 1976 3d Int. Mtg on Theoretical and Experimental Aspects of Heating of Toroidal Plasmas, Grenoble, Vol. 2, p. 305.
11. Namba C. and Kawamura T, 1970, Phys. Lett., 31A, 555.
12. Rose D. J. and Clark M., Jr., 1961, Plasmas and Controlled Fusion, M.I.T. Press.
13. Rothman M. A., Sinclair R. M., Brown I. G., and Hosea J. C., 1969, Phys. Fluids, 12, 2211.
14. Scharer J. E., McVey B. D., Mau T. K., 1976, 3d Int. Mtg. on Theoretical and Experimental Aspects of Heating of Toroidal Plasmas, Grenoble, Vol. 1, p. 79.
15. Sprott J. C., 1969, Ph.D. thesis, U. of Wisconsin.
16. Sprott J. C. and Edmonds P. H., 1971, Phys. Fluids, 14, 2703.

17. Sprott J. C. and Strait E. J., 1976, IEEE Trans. on Plasma Sci., 4, 6.

18. Stix T. H., 1962, Theory of Plasma Waves, McGraw Hill.

19. Swanson D. G., Clark R. W., Korn P., Robertson S., and Wharton C. B., 1972, Phys. Rev. Lett., 28, 1015.

20. TFR Group, 1976, 3d Int. Mtg on Theoretical and Experimental Aspects of Heating of Toroidal Plasmas, Grenoble, Vol. 1, p. 87.

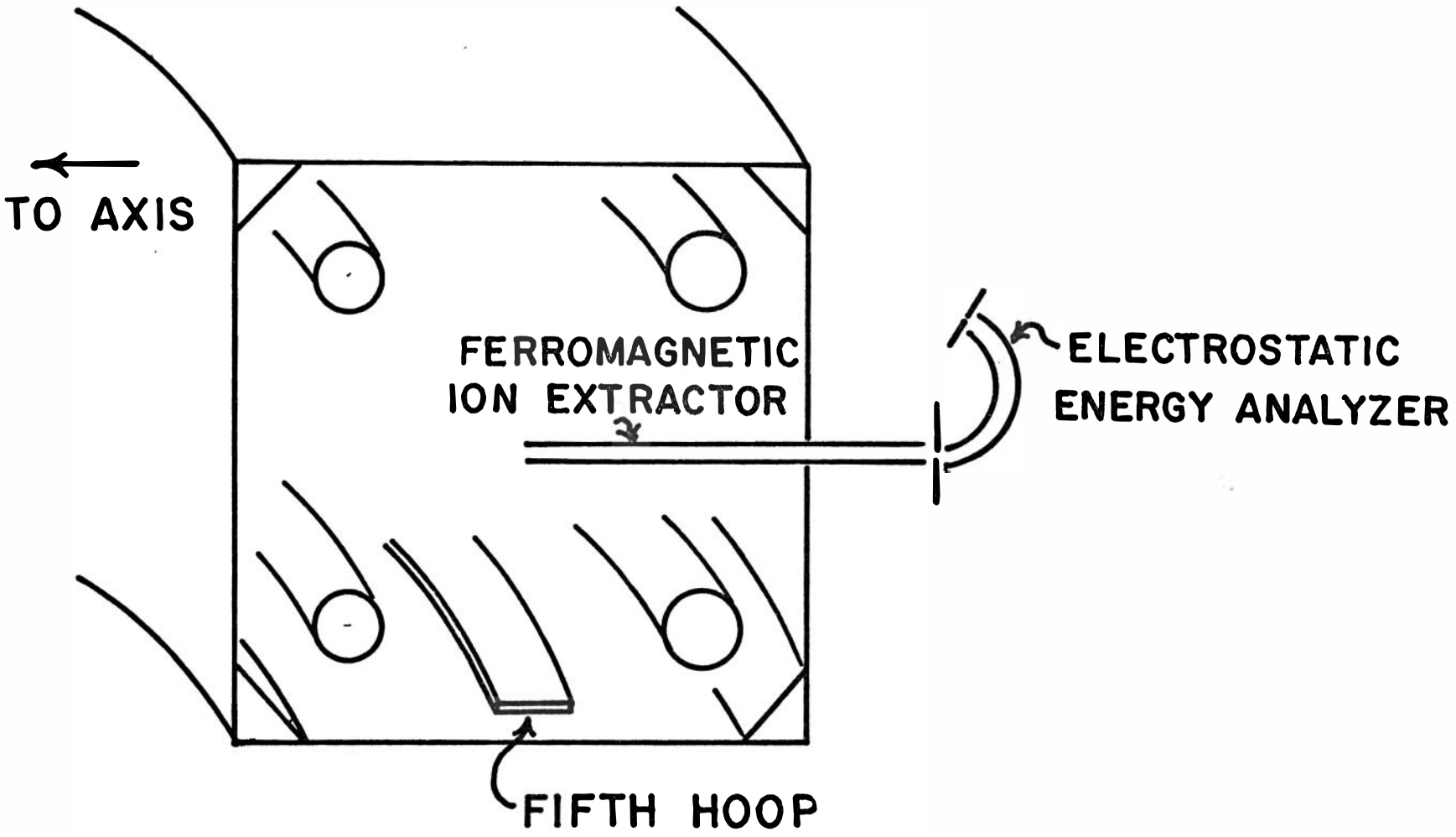
TO AXIS
FERROMAGNETIC
ION EXTRACTOR
ELECTROSTATIC
ENERGY ANALYZER
FIFTH HOOP

FIG 1

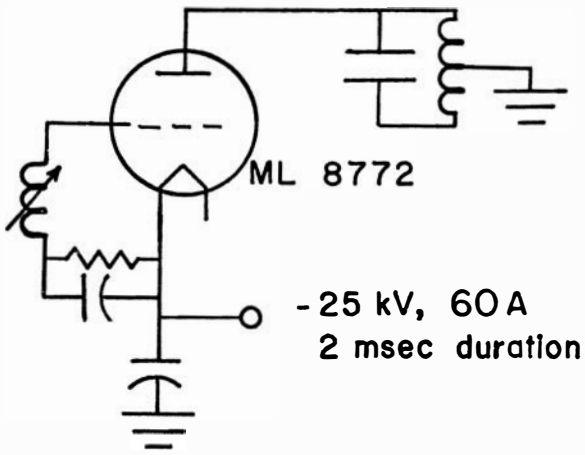

FIG 2

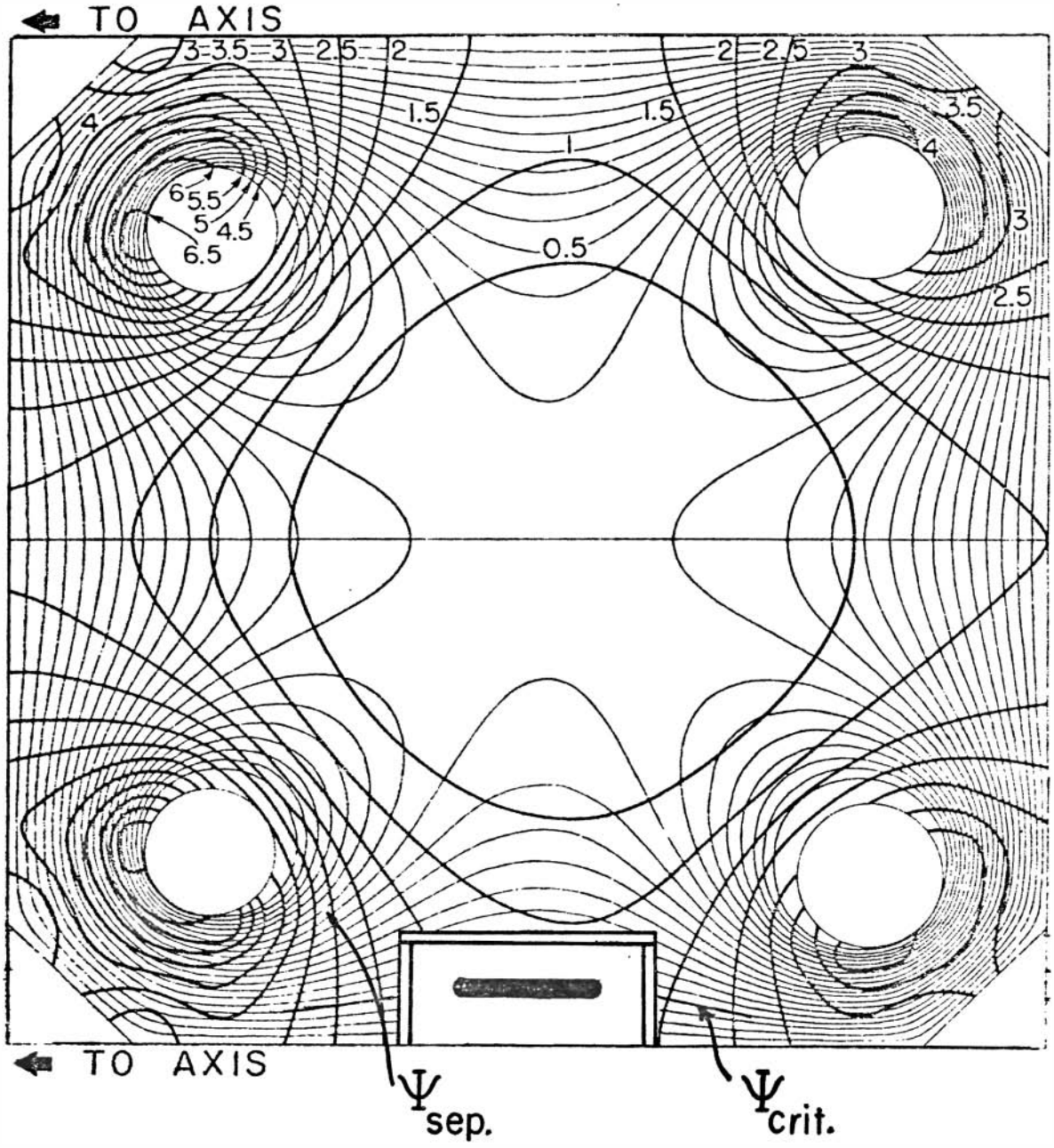
TO AXIS
3
3.5
3
2.5
2
1.5
1
0.5
4
6
5.5
5
4.5
6.5
2
2.5
3
1.5
3.5
4
3
2.5
TO AXIS
$\Psi_{sep.}$
$\Psi_{crit.}$

FIG 3

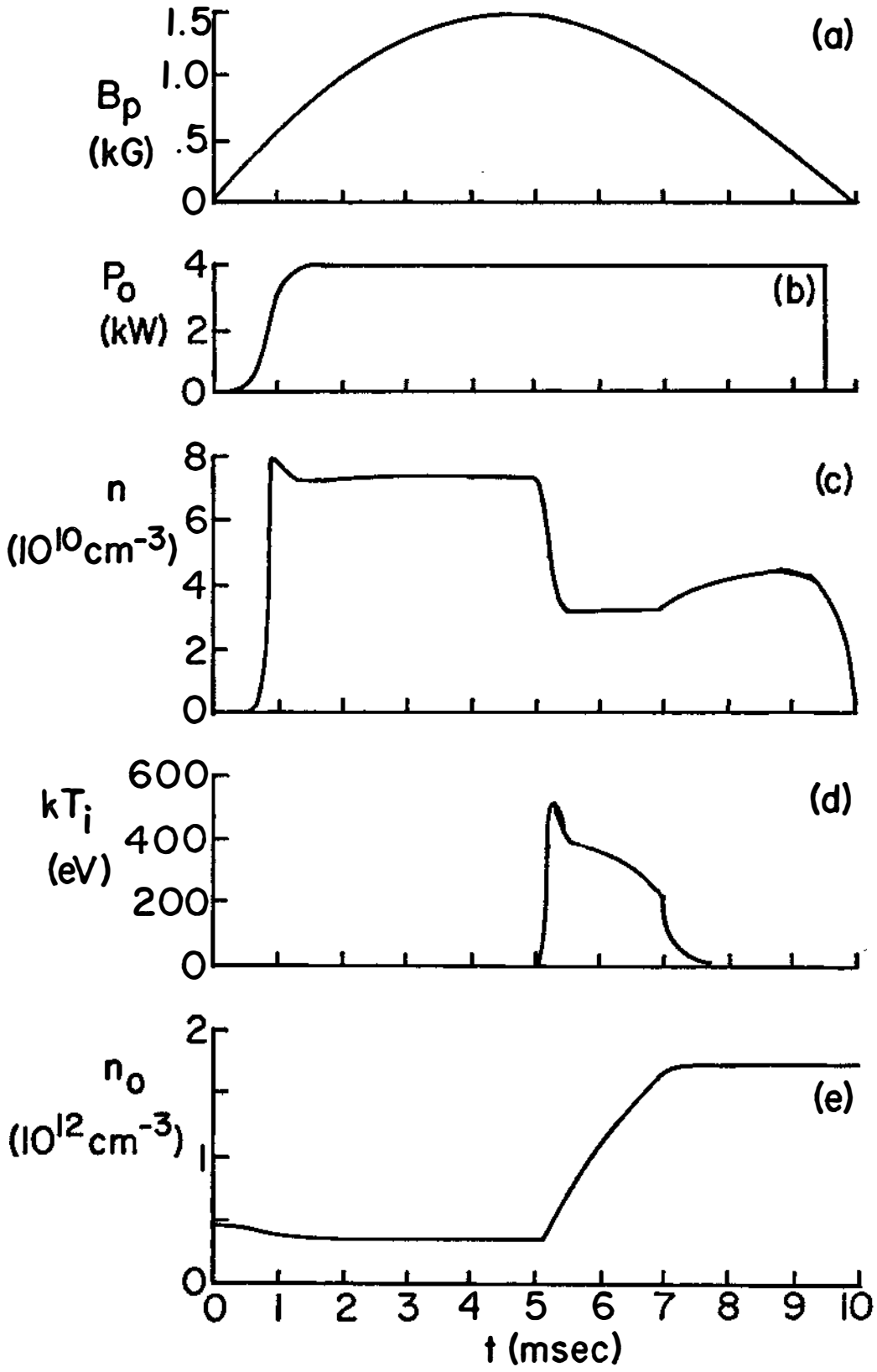
1.5
1.0
.5
0
B_p
(kG)
(a)
4
2
0
P_o
(kW)
(b)
8
6
4
2
0
n
($10^{10}cm^{-3}$)
(c)
600
400
200
0
kT_i
(eV)
(d)
2
1
0
n_o
($10^{12}cm^{-3}$)
(e)
0 1 2 3 4 5 6 7 8 9 10
t (msec)

FIG 4

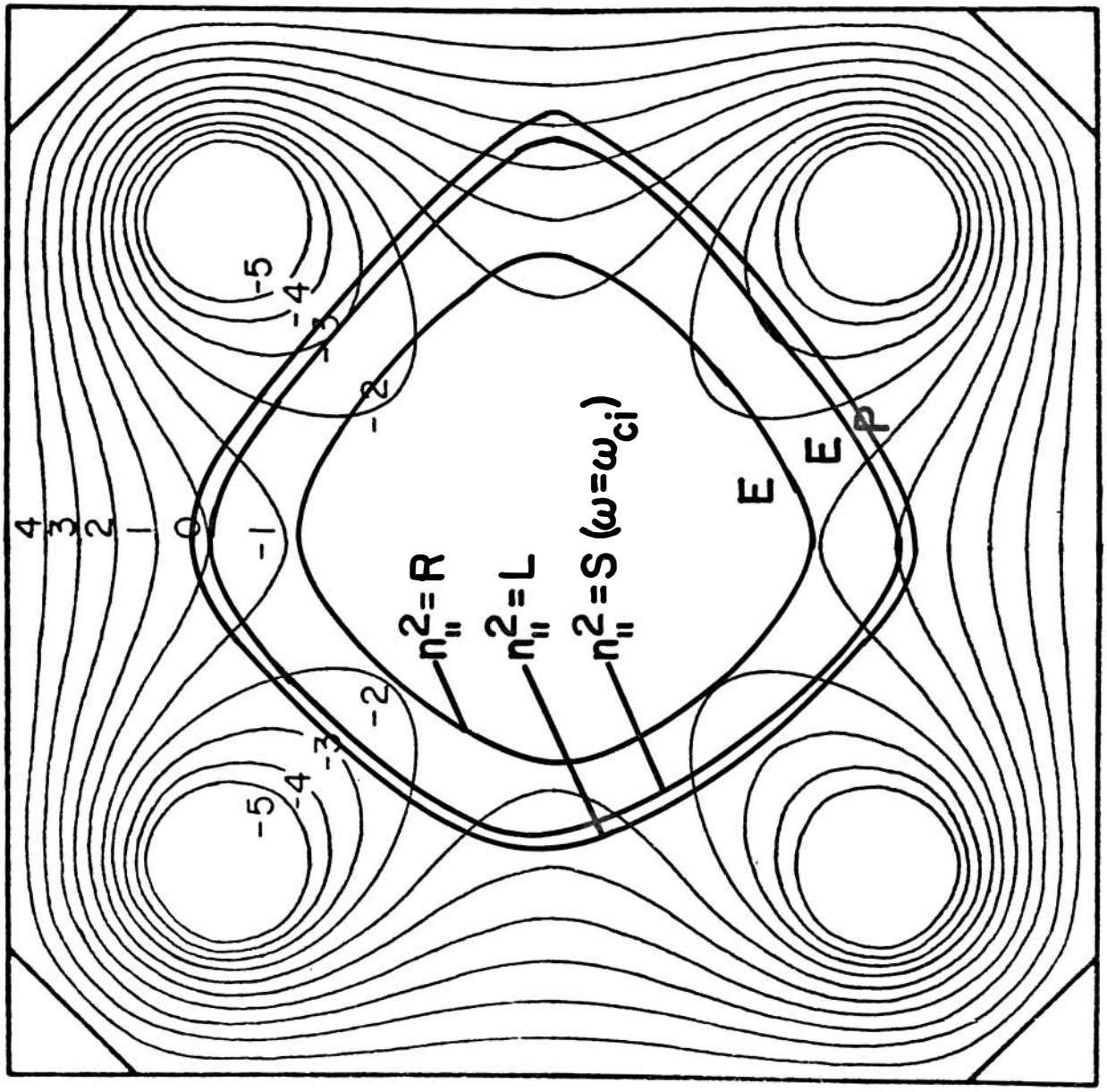
4
3
2
1
0
-1
-2
-3
-4
-5
-5
-4
-3
-2
$n_{\parallel}^2=R$
$n_{\parallel}^2=L$
$n_{\parallel}^2=S\ (\omega=\omega_{ci})$
E
E
P

FIG 5

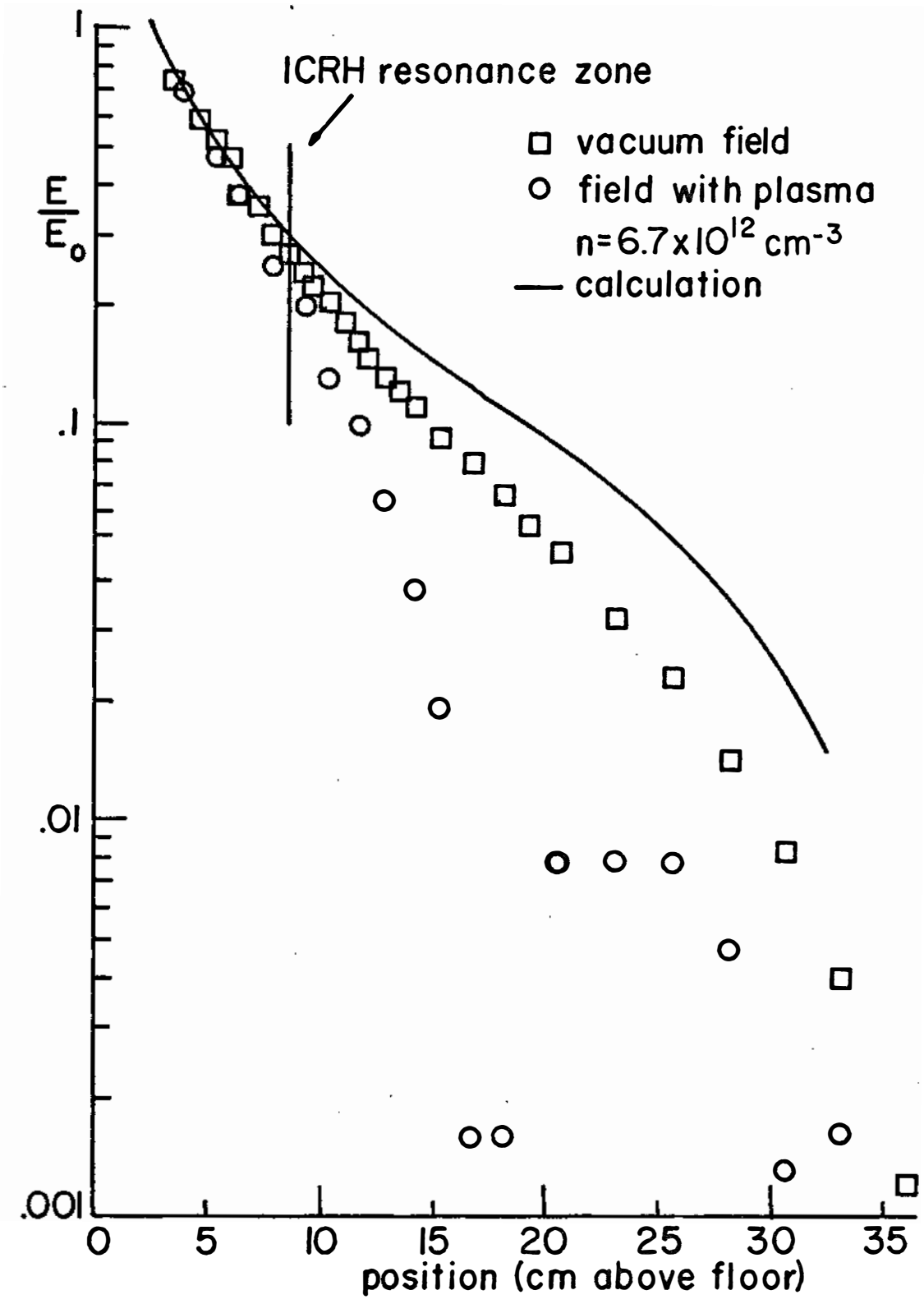
ICRH resonance zone
vacuum field
field with plasma
n=6.7x10^12 cm^-3
calculation
E/E0
1
.1
.01
.001
0
5
10
15
20
25
30
35
position (cm above floor)

FIG 6

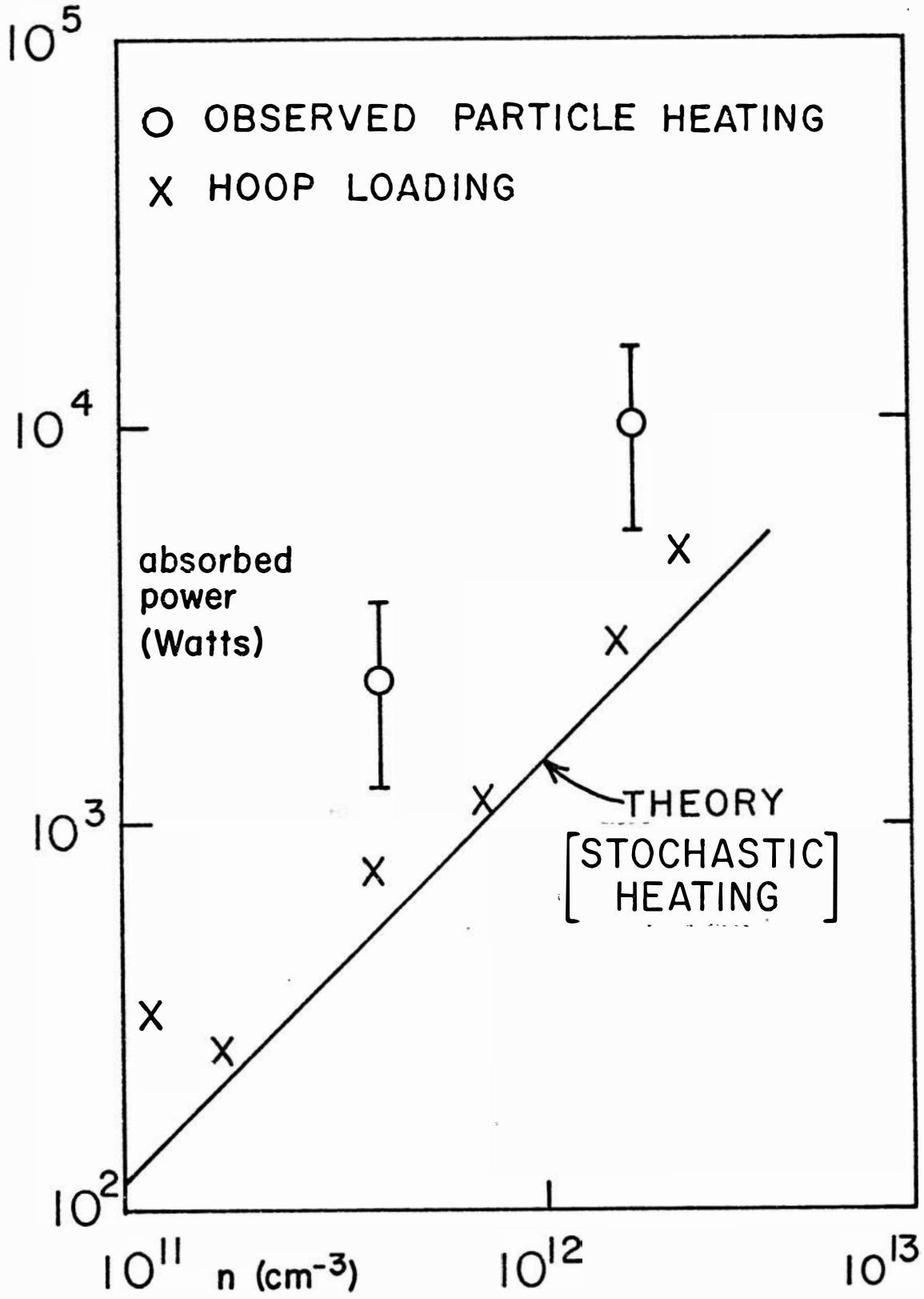
10^5
10^4
10^3
10^2
O OBSERVED PARTICLE HEATING
X HOOP LOADING
absorbed power (Watts)
THEORY
[STOCHASTIC HEATING]
10^{11}
n (cm^{-3})
10^{12}
10^{13}

FIG 7

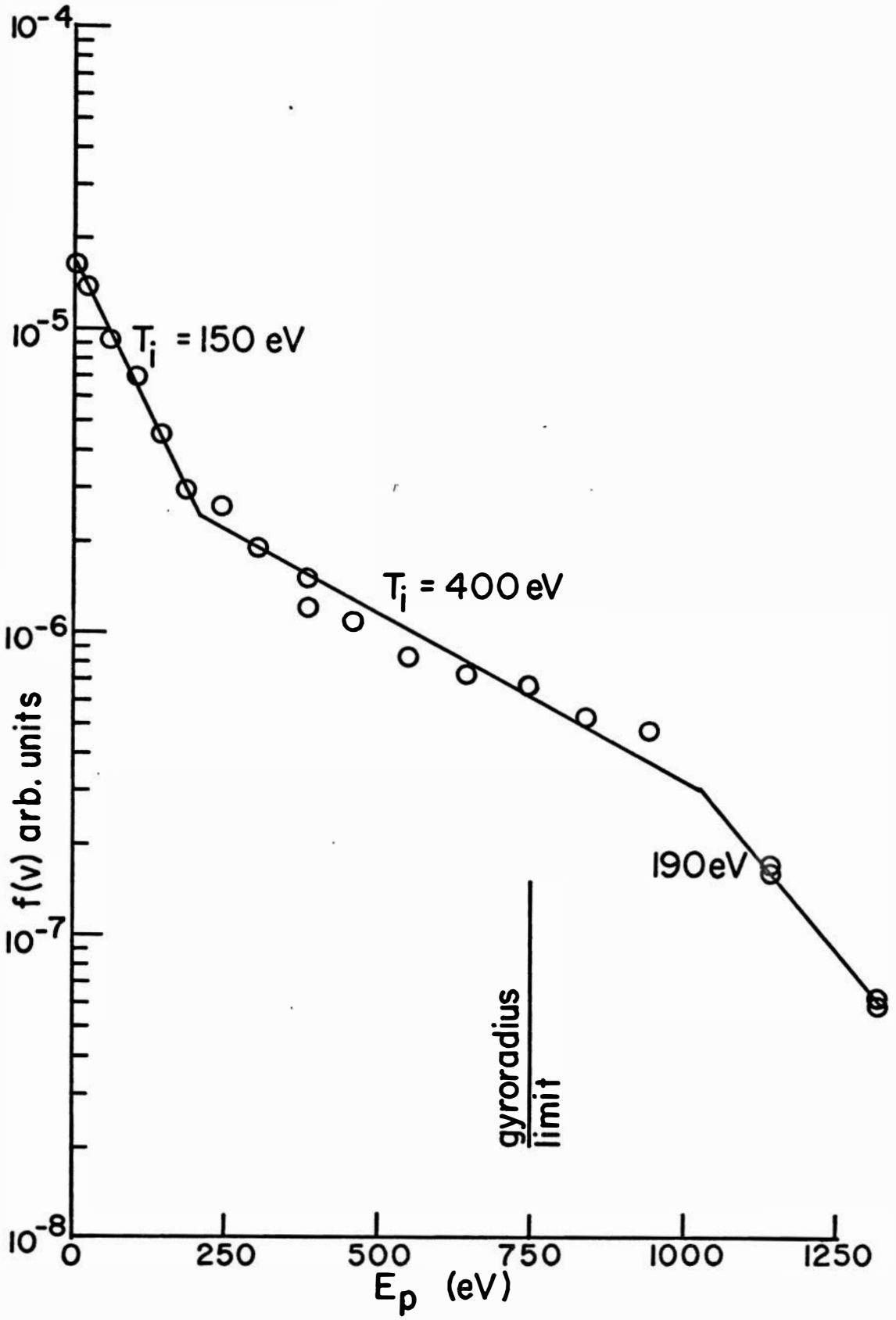
10^-4
10^-5
10^-6
10^-7
10^-8
f(v) arb. units
T_i = 150 eV
T_i = 400 eV
190eV
gyroradius
limit
0
250
500
750
1000
1250
E_p (eV)

FIG 8

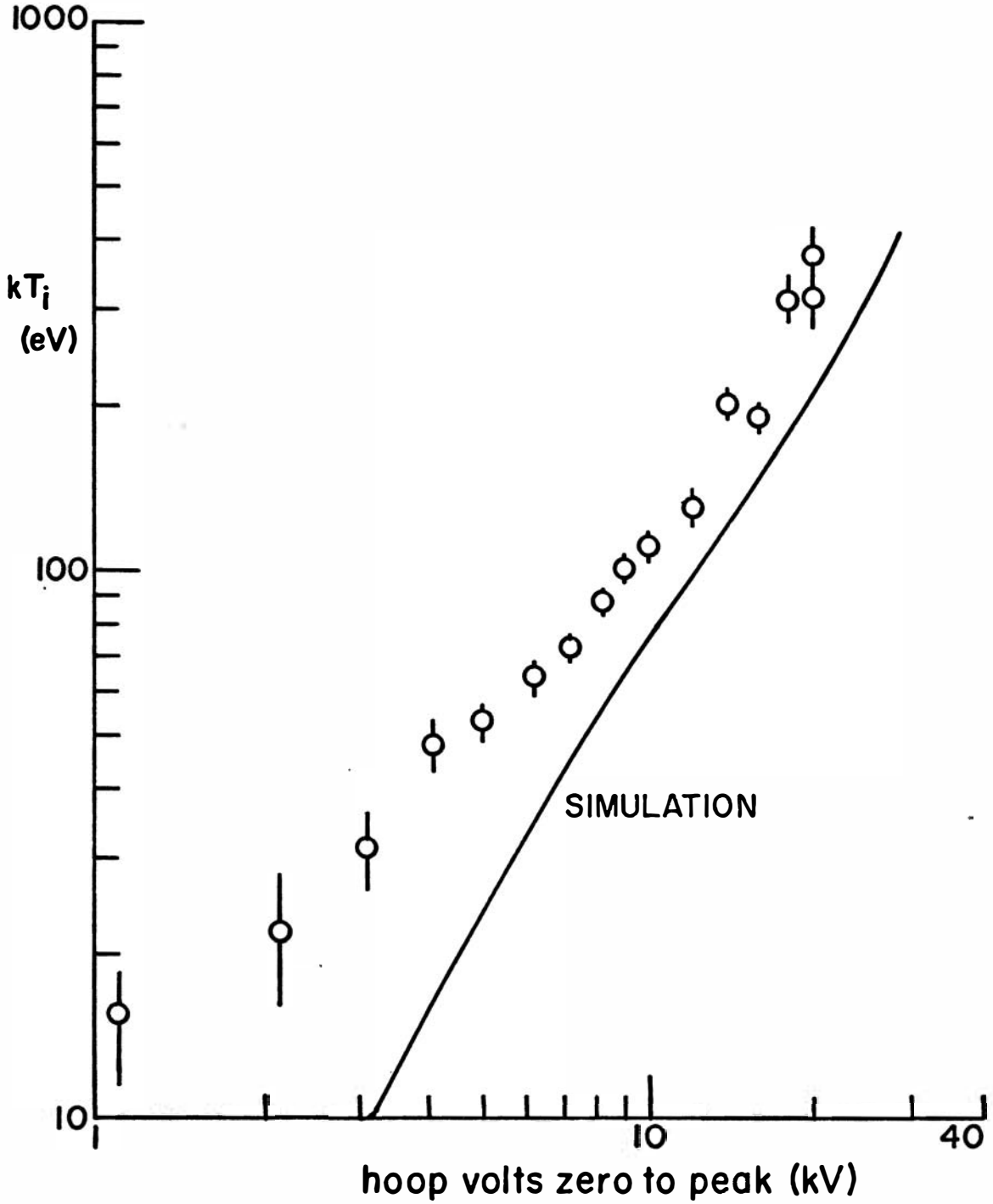
1000
100
10
kT_i
(eV)
SIMULATION
1
10
40
hoop volts zero to peak (kV)

FIG 9

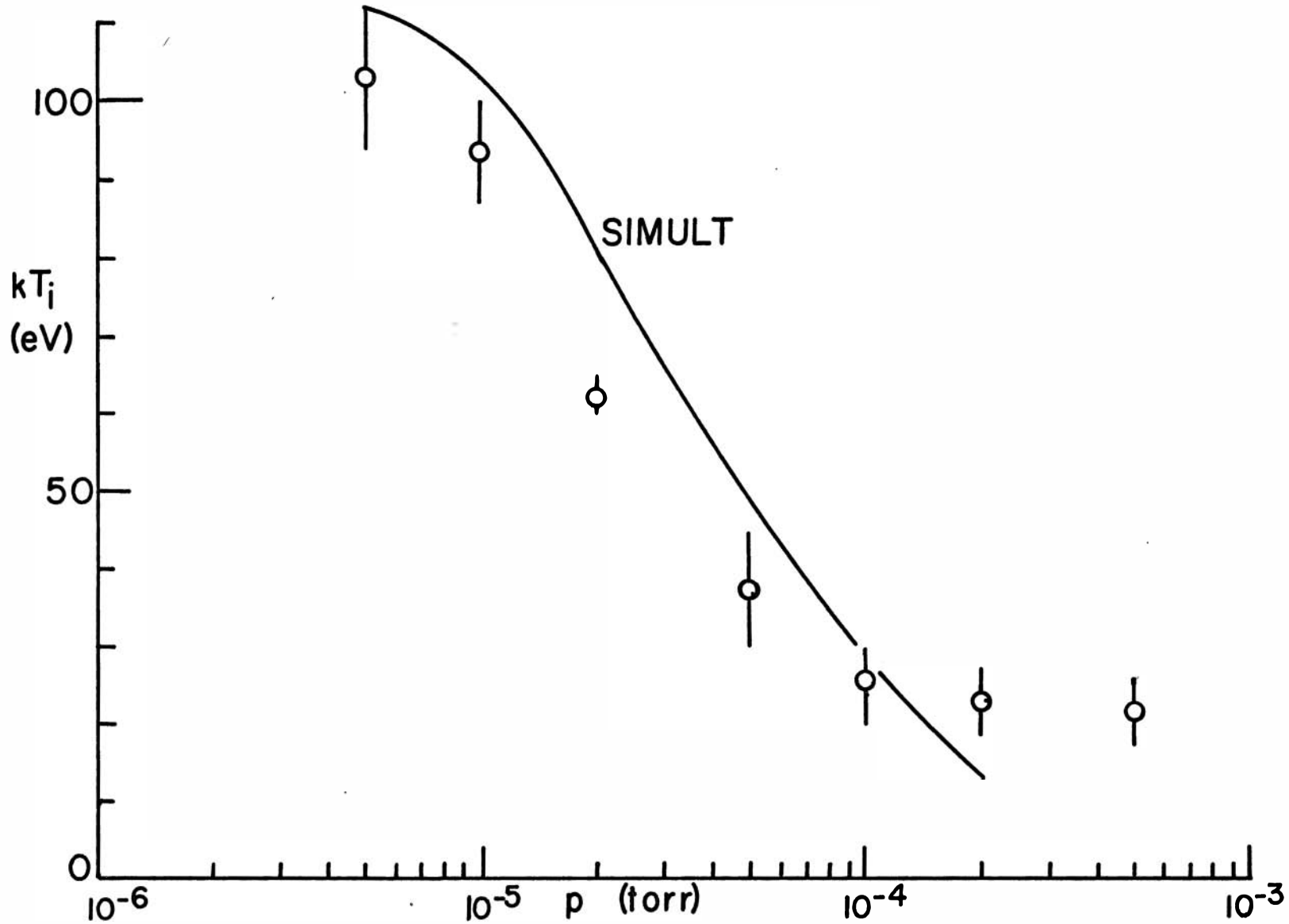

FIG 10

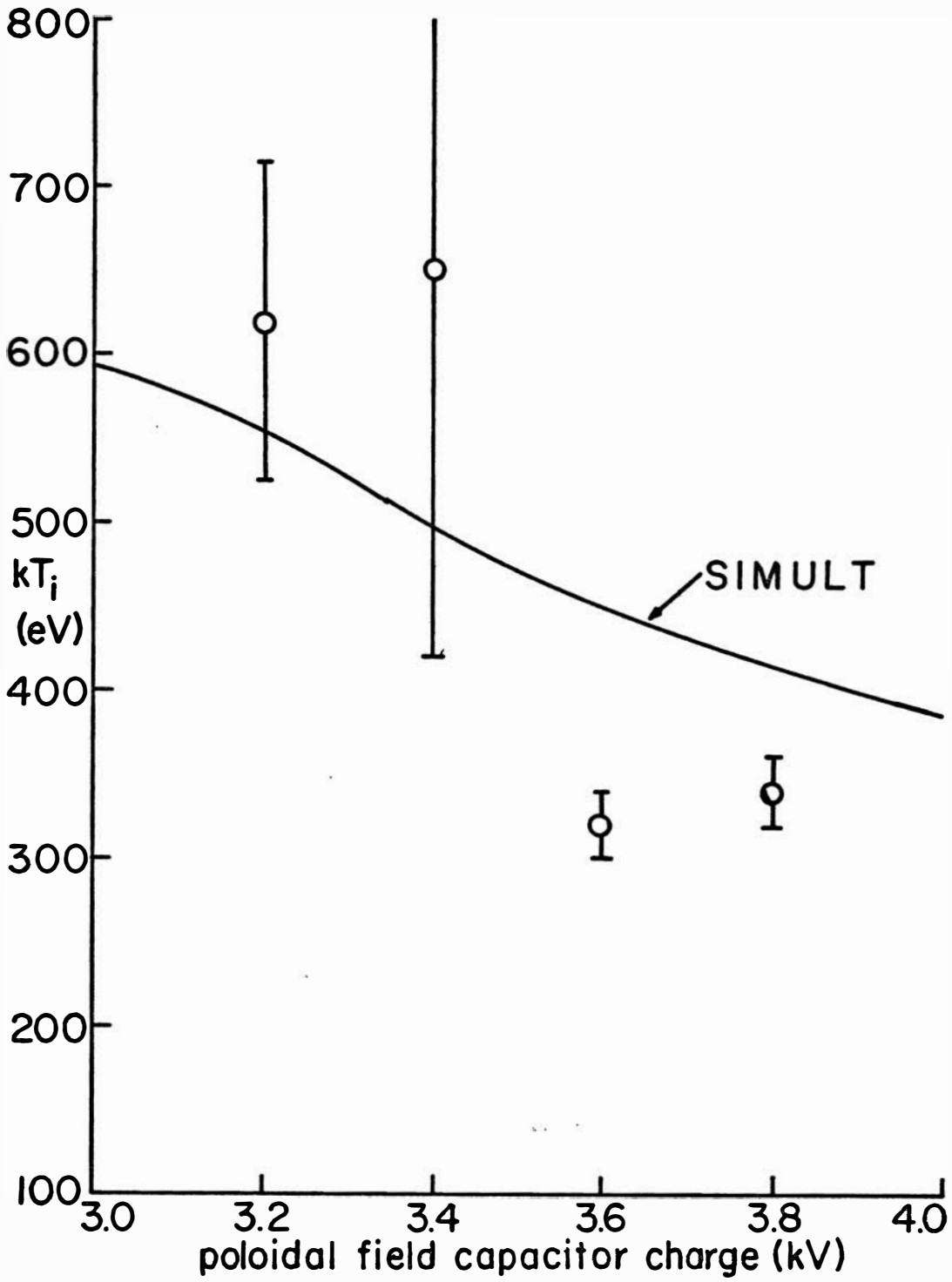
800
700
600
500
400
300
200
100
kT_i
(eV)
SIMULT
3.0
3.2
3.4
3.6
3.8
4.0
poloidal field capacitor charge (kV)

FIG 11

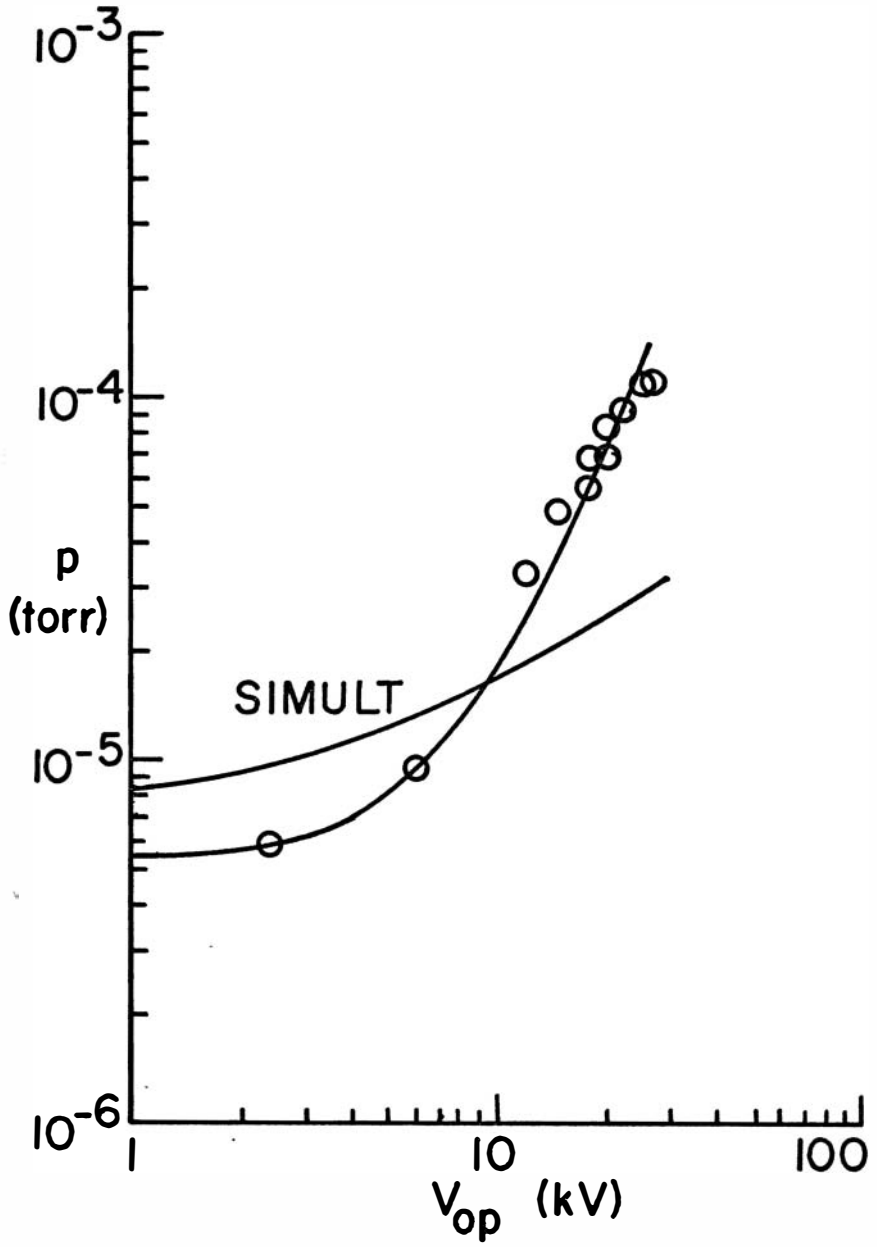

FIG 12

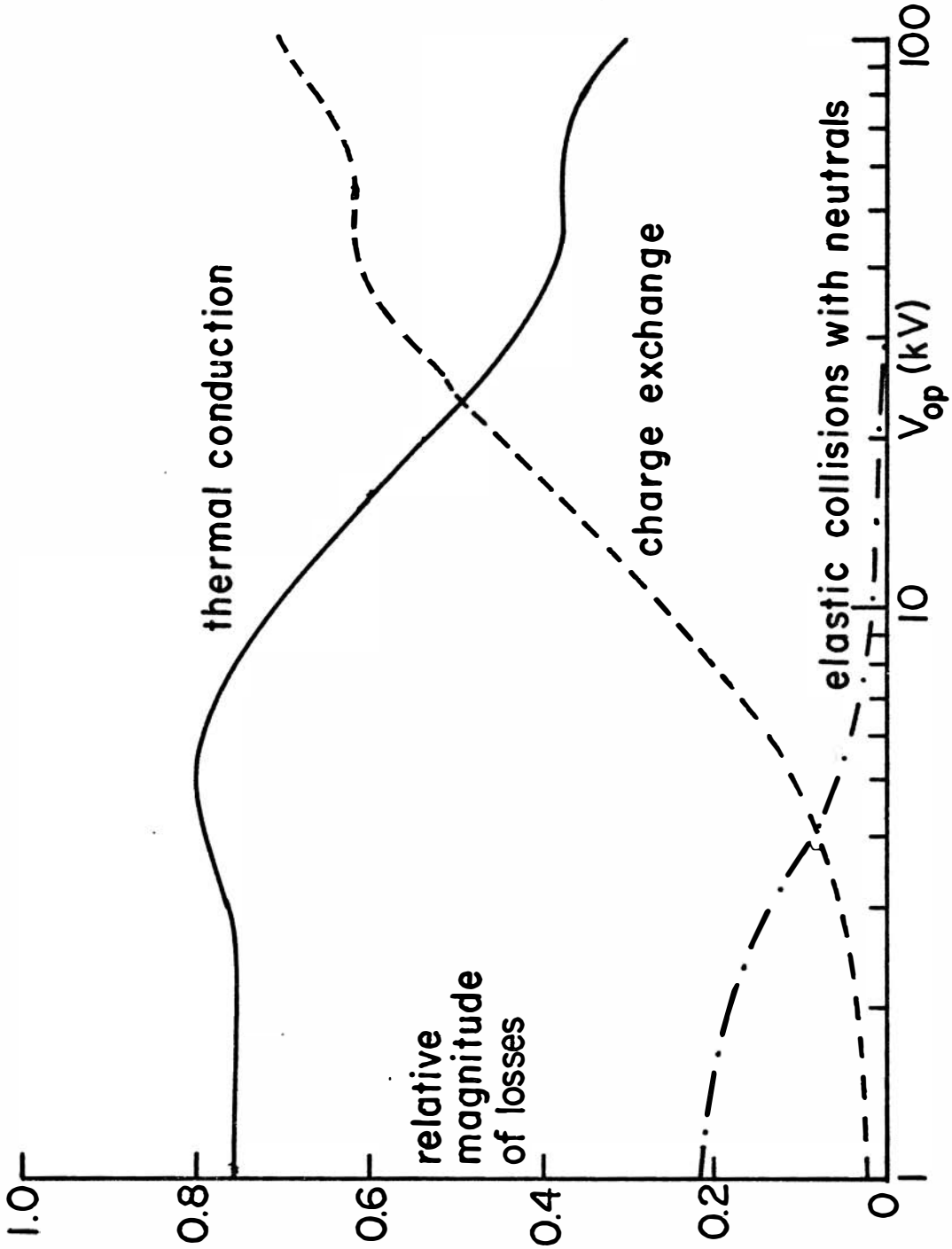
thermal conduction
charge exchange
elastic collisions with neutrals
relative magnitude of losses
1.0
0.8
0.6
0.4
0.2
0
1
10
100
V_{op} (kV)

FIG 13

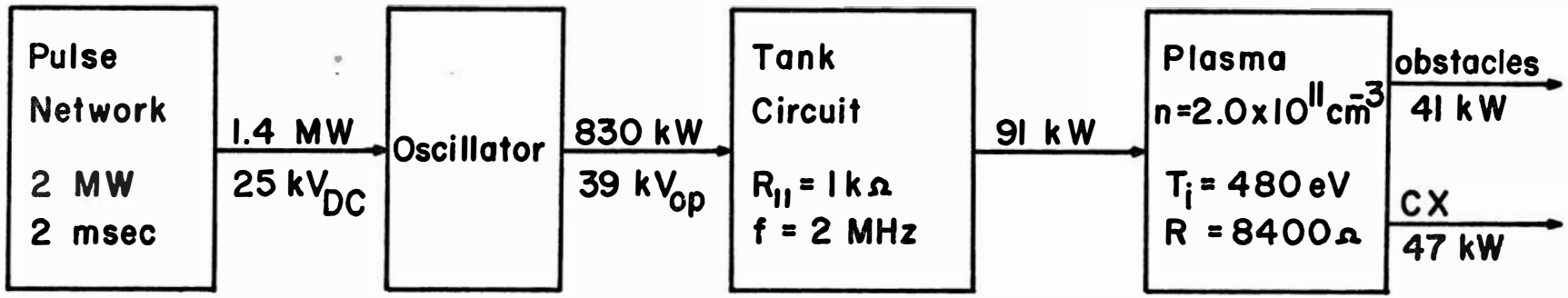

(Center tapped hoop)

F16 14